

Mitochondrial DNA polymorphisms specifically modify cerebral β -amyloid proteostasis

Katja Scheffler · Markus Krohn · Tina Dunkelmann · Jan Stenzel ·
Bruno Miroux · Saleh Ibrahim · Oliver von Bohlen und Halbach ·
Hans-Jochen Heinze · Lary C. Walker · Jörg A. Gsponer · Jens Pahnke

Received: 7 January 2012 / Revised: 1 March 2012 / Accepted: 29 March 2012 / Published online: 18 April 2012
© Springer-Verlag 2012

Abstract Several lines of evidence link mutations and deletions in mitochondrial DNA (mtDNA) and its maternal inheritance to neurodegenerative diseases in the elderly. Age-related mutations of mtDNA modulate the tricarboxylic cycle enzyme activity, mitochondrial oxidative phosphorylation capacity and oxidative stress response. To investigate the functional relevance of specific mtDNA polymorphisms of inbred mouse strains in the proteostasis regulation of the brain, we established novel mitochondrial congenic mouse lines of Alzheimer's disease (AD). We crossed females from inbred strains (FVB/N, AKR/J, NOD/LtJ) with C57BL/6 males for at least ten generations to gain specific mitochondrial conplastic strains with pure

C57BL/6 nuclear backgrounds. We show that specific mtDNA polymorphisms originating from the inbred strains differentially influence mitochondrial energy metabolism, ATP production and ATP-driven microglial activity, resulting in alterations of cerebral β -amyloid (A β) accumulation. Our findings demonstrate that mtDNA-related increases in ATP levels and subsequently in microglial activity are directly linked to decreased A β accumulation *in vivo*, implicating reduced mitochondrial function in microglia as a causative factor in the development of age-related cerebral proteopathies such as AD.

Keywords Abeta · Mitochondrial congenic mice · Conplastic · Alzheimer's disease · Amyloid-beta · Microglia · Mitochondria

Electronic supplementary material The online version of this article (doi:10.1007/s00401-012-0980-x) contains supplementary material, which is available to authorized users.

K. Scheffler · M. Krohn · T. Dunkelmann · J. Stenzel ·
H.-J. Heinze · J. Pahnke
Department of Neurology, Neurodegeneration Research
Laboratory (NRL), Universities of Rostock, Rostock, Germany

M. Krohn · J. Pahnke
German Centre for Neurodegenerative Diseases (DZNE),
Magdeburg, Germany

B. Miroux
Laboratoire de Biologie Physico-Chimique des Protéines
Membranaires, UMR 7099, Institut de Biologie
Physico-Chimique, Paris, France

S. Ibrahim
Department of Dermatology, University of Lübeck,
Lübeck, Germany

O. von Bohlen und Halbach
Institute of Anatomy, University of Greifswald,
Greifswald, Germany

H.-J. Heinze · J. Pahnke
Leibniz Institute for Neurobiology, Magdeburg, Germany

L. C. Walker
Yerkes National Primate Research Center and Department
of Neurology, Emory University, Atlanta, GA, USA

J. A. Gsponer
Center for High-Throughput Biology, University of British
Columbia, Vancouver, Canada

Present Address:

K. Scheffler
Department of Biochemistry, University of Oslo, Oslo, Norway

J. Pahnke (✉)
Department of Neurology, Neurodegeneration Research
Laboratory (NRL), Universities of Magdeburg, Leipziger Str. 44,
H15, 39120 Magdeburg, Germany
e-mail: jens.pahnke@gmail.com
URL: www.NRL.ovgu.de

Introduction

mtDNA mutations become increasingly common throughout the body with advancing age [20] and are thought to be associated with several age-related neurodegenerative disorders [35]. However, there is little compelling evidence linking these mutations to specific pathological changes [6, 22]. Because engineering and integrating specific mutated mtDNA in mice is technically challenging, clinically relevant mouse models with pathological mtDNA mutations are rare [36]. Therefore, naturally occurring mtDNA polymorphisms in common inbred strains hold considerable promise for analyzing the pathogenic effects of polymorphic mtDNA. mtDNA variants interfere with cognitive abilities [30], and differentially modulate mitochondrial oxidative phosphorylation (OXPHOS) and the generation of reactive oxygen species (ROS) [26]. The age-related decline of respiratory chain function in mtDNA-mutant mice was found to be more strongly affected by mtDNA point mutations than by deletions [11]. Numerous findings also implicate mitochondrial dysfunction and oxidative damage in the pathogenesis of neurodegenerative diseases, such as Alzheimer's disease (AD) [24]. For instance, depleting cells of endogenous mtDNA in vitro and repopulating them with mitochondria from AD patients resulted in respiratory chain deficiency and β -amyloid (A β) accumulation [18, 33]. Sequencing of mtDNA from the blood or brain tissue of AD patients however yielded contradictory results [12, 34]. Hence, the hypothesized connection between specific mtDNA polymorphisms and defects in protein maintenance (protein homeostasis or proteostasis), specifically the cerebral accumulation of A β , remains uncertain [9, 10].

Materials and methods

Animal models and generation of congenic mouse lines

(1) APP-transgenic mice [29] (C57BL/6 gDNA and mtDNA background) were obtained from R. Radde and M. Jucker (University of Tübingen, Hertie Institute for Clinical Brain Research, Tübingen, Germany) and further maintained with C57BL/6 females for more than six generations (APP-B6). C57BL/6 female mice (B6) were purchased from Jackson Laboratory (Bar Harbor, ME, USA). (2) APP-FVB mice were generated by crossing APP-transgenic mice to FVB/N females for more than ten generations. FVB/N female mice were purchased from the Jackson Laboratory. (3) Mouse inbred strains (FVB/N, AKR/J, NOD/LtJ) used to generate mtDNA conplastic strains were purchased from Jackson Laboratory. The mtDNA of each strain had been sequenced previously [38].

C57BL/6 (B6) was chosen as the gDNA and mtDNA reference strain because the APP-transgenic mouse model on the same background is well characterized [29, 31]. Based on the exclusive inheritance of maternal mtDNA [1], we mated female mice manifesting the desired mtDNA variants with male B6 mice for more than ten generations to eliminate the nuclear DNA of the inbred strains AKR/J, FVB/N, and NOD/LtJ, respectively. APP-B6 males (Sect. 1 above) were then crossed to mtDNA strains to produce APPxmt^{AKR}, APPxmt^{FVB} and APPxmt^{NOD} mice, respectively. (4) Uncoupling protein 2-knockout mice (*Ucp2*^{0/0}, C57BL/6 gDNA and mtDNA background) were provided by Bruno Miroux. APP-B6 mice were crossed to *Ucp2*^{0/0} mice to produce APP⁺⁰xUCP2^{0/0} mice.

All mice were housed in a climate-controlled environment on a 12 h light/dark cycle with free access to rodent food (SNIFF, Germany) and water. All procedures were conducted in accordance with animal protocols approved by the University of Rostock and according to the state law of the government of Mecklenburg-Western Pomerania.

Tissue preparation

Mice were killed by cervical dislocation and transcardially perfused with PBS. The brain was removed, and one hemisphere was fixed in buffered, 4 % paraformaldehyde (PFA) for paraffin-embedding and immunohistochemistry, while the other hemisphere was snap-frozen in liquid nitrogen and stored at -80°C for biochemical analysis.

Enzyme-linked immunosorbent assay (ELISA)

ELISA kits (TK42HS—high sensitivity from The Genetics Company, Schlieren, Switzerland) were used for the quantification of A β 42 in whole brain hemispheres from which the cerebellum and brain stem had been removed at the level of the midbrain. Hemispheres were homogenized using PreCellys24 (12 s, 6,500 rpm). After addition of carbonate buffer (pH 8.0), homogenates were mixed using PreCellys (5 s, 5,000 rpm) and centrifuged for 90 min (4°C) at 24,000g to separate insoluble from soluble A β species. The resulting supernatant (buffer-soluble fraction) was mixed with 8 M guanidine hydrochloride at a ratio of 1:1.6. To extract aggregated A β species, the pellet was dissolved in 8 volumes of 5 M guanidine hydrochloride, shaken at room temperature for 3 h and centrifuged at 24,000g for 20 min at 4°C . The resulting supernatant represents the guanidine-soluble fraction. Protein contents of all samples were measured in triplicate using a Nano-drop1000 (Thermo Fisher Scientific, USA). ELISAs were performed according to the manufacturer's instructions using appropriate dilutions.

TCA and OXPHOS activity measurements in isolated mitochondria

Mitochondria from freshly prepared brain hemispheres were isolated as described elsewhere [38]. The mitochondria were adjusted to the same protein concentration as determined by BCA assay (Pierce, a division of Thermo Fisher Scientific, USA). The different enzymatic activities were assessed using the PARADIGM spectrophotometer (Beckman Coulter, USA). Pyruvate DH activity was measured using a PDH enzyme activity microplate assay kit (MitoScience, USA). Malate DH activity was measured by monitoring the absorbance at 340 nm in a reaction mixture containing 50 mM potassium phosphate buffer (pH 7.4), 0.4 mM NADH, 2 mM oxaloacetate and 10 μ M rotenone. Complex I, III and ATPase activities were measured as described elsewhere [2, 38]. The ATPase activity represents complex V activity. Complex II and IV activities were measured using the respective enzyme activity microplate assay kits (MitoScience, USA).

Assessment of ATP and H₂O₂ levels

ATP and H₂O₂ levels were measured in freshly prepared total brain homogenates. Assays were performed with either a luminescence (Infinite200Pro, Tecan, Switzerland) or spectrophotometric plate reader (PARADIGM, Beckman Coulter, USA). Tissue ATP levels were determined by a luciferin/luciferase ATP Bioluminescent Assay kit (Sigma-Aldrich, Germany). The Amplex Red hydrogen peroxide assay kit (Invitrogen, USA) was used to detect H₂O₂ release. Sample preparation and assay procedures were performed according to the manufacturers' protocols. Due to the high activities of ATPases in fresh samples, tissue was immediately snap frozen in liquid nitrogen. All steps for sample preparation were carried out at 4 °C in order to avoid the recovery of ATPase activity and subsequently degradation of ATP in the tissue.

Catalase and β -secretase activity measurements

Enzyme activities were measured in total brain homogenates. The different enzymatic activities were assessed using the PARADIGM spectrophotometer (Beckman Coulter, USA). Catalase activity was measured by using an OxiSelect catalase activity assay kit (Cell Biolabs, USA). The activity of β -secretase was determined with a β -secretase activity assay kit (BioVision, USA). Sample preparation and assay procedures were performed according to the manufacturers' protocols.

Western blots

For Western blotting, tissue homogenates were prepared as described by Lesné et al. [23]. Total protein concentrations of the extracts were determined using a BCA assay (Pierce, division of Thermo Fisher Scientific, USA). After electrophoresis of 10 μ g total protein per lane, proteins were blotted onto PVDF membranes. After blocking in 5 % dry milk in TBST buffer (50 mM Tris pH 7.4, 150 mM NaCl, 0.1 % Tween20) for 1 h at room temperature, blots were probed for ADAM10 (1:1,000, Calbiochem, USA), BACE1 (1:1,000, Abcam, UK), IDE (1:500, Abcam, UK), ApoE (1:2,000, Abcam, UK), ABCA1 (1:1,000, Novus Biologicals, USA), total OXPHOS antibody cocktail (1:1,000, MitoSciences, USA) or β -actin (1:40,000, Sigma-Aldrich, Germany) overnight at 4 °C. As detection antibodies, anti-mouse-HRP and anti-rabbit-HRP, respectively, were used. The Amersham ECL Plus Detection kit (GE Healthcare, UK) and a Roper CoolSnap HQ² Camera (Roper, Germany) were used for visualization.

Immunohistochemistry

Brain hemispheres were post-fixed for at least 24 h in buffered, 4 % paraformaldehyde. Paraffin-embedded, 4- μ m-thick coronal sections were stained using a BondMaxTM (Leica Microsystems GmbH, Germany) automated immunostaining system. Sections were pretreated with 98 % formic acid for 5 min and immunostained for A β using the anti-human A β clone 6F3D (1:200, 30 min, DAKO, Germany) and the BondTM Polymer Refine Detection kit (Leica Microsystems GmbH, Germany). For double-stained slides, microglia were subsequently immunostained on the same sections using anti-Iba1 (1:1,000, 30 min, Wako GmbH, Germany) and the BondTM Polymer AP-Red Detection kit (Leica Microsystems GmbH, Germany) [31]. Whole tissue sections were fully digitized at a resolution of 230 nm using Mirax Desk/Midi slide scanners (Zeiss, Germany) and then analyzed semi-automatically using the AxioVision software package (Zeiss Microimaging GmbH, Germany) as previously described in [31].

Primary microglia preparation and A β -phagocytosis assays

Highly purified primary microglial cultures were prepared as described by Horvath et al. [15] with slight modifications. In brief, cerebral cortices of 2- to 3-day-old mice were minced and digested with 1 \times Trypsin/EDTA for 15 min at 37 °C. Pelleted tissue was triturated several times on ice in Dulbecco's modified Eagle's medium supplemented with 10 % FBS, 1 % GlutaMax, 1 % penicillin/streptomycin and 2,000 units of DNase. Supernatant containing glial cells was collected, triturated again until

the tissue clumps disappeared and finally centrifuged at 340g for 15 min. The cell pellet was re-suspended in media and plated at 2×10^6 cells per 75 cm² flask. Cultures were maintained at 37 °C and 5 % CO₂. Media were changed every 3–4 days. After 20 days in culture, the flask was shaken at 250 rpm for 45 min, and the primary microglia-enriched supernatant was removed and centrifuged at 340g for 15 min. To assess the phagocytosis of A β , the cell pellet was resuspended in media and plated at 30,000 primary microglia per well onto a 96-well plate. Peptide phagocytosis was quantified by measuring the uptake of FITC-labelled A β 42 (rPeptide, USA). A β aggregates (500 nM) were incubated with the microglia for 6 h. Then the medium was removed and the remaining cells were washed twice with PBS and trypsinized. The cells were centrifuged at 340g for 15 min and resuspended in PBS. Intracellular fluorescence (excitation 485 nm and emission 535 nm) was measured with the PARADIGM spectrophotometer (Beckman Coulter, USA).

Immunofluorescence

Primary microglia were seeded at 200,000 cells per 6-well plate onto poly-D-lysine-coated cover slips. After 24 h incubation with 500 nM FITC-labeled A β 42, cells were fixed with 2 % paraformaldehyde for 5 min and then ice-cold methanol for an additional 5 min. Primary microglia were immunolabelled using an antibody against Iba1 (1:1,000, Wako GmbH, Germany) for 1 h. Detection was performed with goat anti-rabbit Cy3 (1:1,000, Dianova, Germany). Cells were counterstained and mounted using VECTASHIELD with DAPI (Biozol, Germany). Visualization was achieved with a Zeiss Laser Scanning Microscope (LSM700, Zeiss, Germany).

Results

Inbred AD mouse strains show distinct differences in A β load

Support for a link between DNA polymorphisms and altered protein homeostasis comes from the initial evaluation of the influence of the C57BL/6J (B6) and FVB/N murine strain backgrounds on cerebral A β accumulation in APP-transgenic mice. B6 and FVB/N mice differ substantially in nuclear and mitochondrial DNA. ELISA quantifications revealed significantly lower A β levels in APP-FVB mice compared to APP-B6 mice at 200 days of age (Fig. 1). This indicates that nuclear and/or mitochondrial DNA variations may cause these differences while expressing the identical APP transgenes.

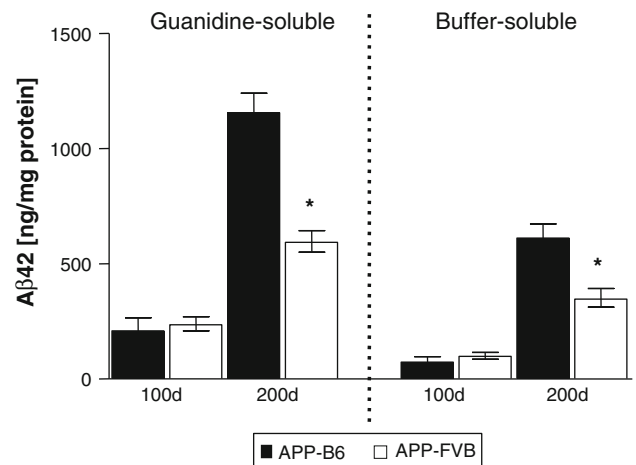


Fig. 1 Strain-specific difference in A β concentrations. ELISA measurements of A β 42 in APP-transgenic mouse models in two different background strains demonstrate significantly reduced A β 42 levels in both the guanidine-soluble and buffer-soluble fractions in APP-FVB inbred mice at 200 days of age. Data are presented as means \pm SEM ($n \geq 5$ per group), * $p < 0.05$

Conplastic mice show distinct biochemical differences

To determine whether the observed differences in A β levels are indeed caused by mtDNA differences between B6 and FVB/N, we established new mtDNA congenic AD mouse lines by using common inbred strains (FVB/N, AKR/J, NOD/LtJ) with naturally occurring mtDNA polymorphisms leading to coding and non-coding nucleotide exchanges (Table 1). As mitochondria are inherited maternally, we backcrossed female mice of these strains for at least ten generations with B6 males to gain solely mitochondrial differences on an otherwise pure B6 background (B6xmt^{AKR/J}, B6xmt^{FVB/N}, and B6xmt^{NOD/LtJ}). The offsprings after the tenth generation were regarded as congenic/conplastic strains that carried the nuclear genome of the recipient strain and the mitochondrial genome from the donor strains. The resulting congenic mtDNA mice were then crossed to APP-B6 males to evaluate intracerebral A β proteostasis in the context of variant mtDNA (conplastic AD mice: APP-B6xmt^{FVB/N} [mt^{FVB}], APP-B6xmt^{AKR/J} [mt^{AKR}], APP-B6xmt^{NOD/LtJ} [mt^{NOD}]).

Sequencing the mtDNA of these common inbred strains revealed four genetic variants (Table 1): (1) a poly A insertion in the D-loop of *mtRNA*^{Arg} in all three mtDNA congenic mouse strains previously described to alter not only hearing ability in mice, but also to differentially affect ROS production in transmitochondrial cybrids [17, 26]; (2) a coding substitution in the ATP synthase subunit 8 (*Atp8*) gene in the mt^{FVB} DNA, altering mitochondrial function [38]; (3) a coding substitution in the cytochrome c oxidase subunit 3 (*Cox3*) gene in mt^{NOD} mice, leading to decreased complex IV activity (Supplementary Fig. 2); (4) a non-

Table 1 mtDNA sequence variation among the four inbred mouse strains

Position (bp)	C57BL/6J	AKR/J	FVB/N	NOD/LtJ	Gene/RNA	Amino acid substitution
7778	G	G	T	G	<i>mt-Atp8</i>	Asp → Tyr
9348	R	G	G	A	<i>mt-Cox3</i>	Val → Ile
9461	T	C	C	C	<i>mt-Nd3</i>	None
9828	A	AA	AA	AAA	<i>mtRNA^{Arg}</i>	

C57BL/6J was set as the reference strain. Shown are nucleotide positions of mtDNA-encoded genes at which differences occur (indicated in bold letters)

coding substitution in the NADH dehydrogenase subunit 3 (*Nd3*) gene in all three mtDNA congenic mouse strains. The relevance of non-coding single nucleotide exchanges in the NADH dehydrogenase gene is as yet unknown; however, transcriptional regulation of NADH dehydrogenase subunits has been discussed in the context of proteostasis defects [5].

To evaluate the impact that the mtDNA variants have on cellular metabolism, we first analyzed the enzymatic activities of the components of the respiratory chain complex, the tricarboxylic acid cycle (TCA) and the resulting cellular ATP levels in the brain. In all mtDNA mouse strains, we found significant differences in TCA enzymes and OXPHOS complex activities (Supplementary Figs. 1, 2) that ultimately resulted in significantly increased ATP levels in *mt^{NOD}* mice (+75 %), and non-significantly in *mt^{AKR}* mice (+35 %) and in *mt^{FVB}* mice (+52 %, Fig. 3a). Because ROS production differs in relation to murine mitochondrial DNA haplotypes [26], we then measured hydrogen peroxide (H₂O₂) levels and catalase activity in the conplastic AD mice. H₂O₂ levels were reduced only in the *mt^{FVB}* strain (−48 %), whereas catalase activity was unchanged in all mtDNA strains and B6 controls (Supplementary Fig. 3). Overall these results demonstrate that single nucleotide differences in the mtDNA can cause substantial metabolic changes.

Conplastic mice exhibit differences in Aβ load

To reveal which impact these metabolic changes have on cerebral proteostasis, we quantified Aβ in the conplastic AD strains. Immunohistochemical analysis showed that Aβ-immunoreactive senile plaques were reduced both in size and number in all mtDNA conplastic strains compared to the APP-B6 controls (Fig. 2a–g). Quantification of cortical plaques in progressively older age groups of mice showed that *mt^{NOD}* mice had a lower areal density of plaques evident as early as at 75 days of age, whereas plaque load in the other groups (*mt^{AKR}*, *mt^{FVB}*) was similar to controls until 175 days of age. At 200 days of age, plaque load was significantly lower in all mtDNA-variant mice (Fig. 2h). These findings were confirmed by ELISA

measurements in which Aβ levels were significantly lower in the mtDNA variant mice (−59 % *mt^{AKR}*, −65 % *mt^{FVB}*, −82 % *mt^{NOD}*) (Fig. 2i). Again, lower Aβ levels were apparent in the *mt^{NOD}* mice as early as 75 days of age (Fig. 2i and Supplementary Fig. 4). To exclude that the differences in Aβ deposition are due to alterations in APP processing pathways, we measured the levels of several proteins/proteases involved in the production, degradation or trafficking of Aβ. The expression of α-secretase (ADAM10), β-secretase (BACE1), ABCA1, ApoE or IDE did not differ as a function of mitochondrial status. In addition, β-secretase activity did not differ significantly among the mouse strains as determined at 200 days of age (Supplementary Fig. 5). These results reveal that other mechanisms are likely involved in the changed Aβ proteostasis.

Microglia function is regulated by conplastic mitochondria

Activated microglial cells rely strongly on mitochondrial function; they are a prominent feature of Aβ plaques and are known to be involved in the phagocytosis of Aβ [14, 28]. Thus, we were interested whether the mtDNA polymorphisms result in variations of the cerebral proteostasis due to changes in microglial activity. We found severe microgliosis in mtDNA-variant mice at 200 days of age, most prominently in the *mt^{NOD}* mice (Fig. 3c–f). All conplastic strains exhibited significantly greater numbers of Aβ plaques that were heavily covered (>50 %) by microglia at day 100 (+128 % *mt^{AKR}*, +153 % *mt^{FVB}* and +186 % *mt^{NOD}*), whereas only *mt^{NOD}* mice maintained a significantly elevated microglial response at 200 days of age (+93 %, the endpoint of our analysis) (Fig. 3b). To assess the potential association between microglial mtDNA polymorphisms and the number and size of Aβ plaques, we studied the phagocytosis of Aβ by microglia in vitro. Immunofluorescence analysis of Iba1-positive microglia isolated from mtDNA mice and B6 controls incubated with fluorescein-coupled Aβ42 revealed an intravesicular localization of Aβ aggregates (Fig. 3g). Quantification of Aβ phagocytosis in *mt^{NOD}* mice, which show the lowest

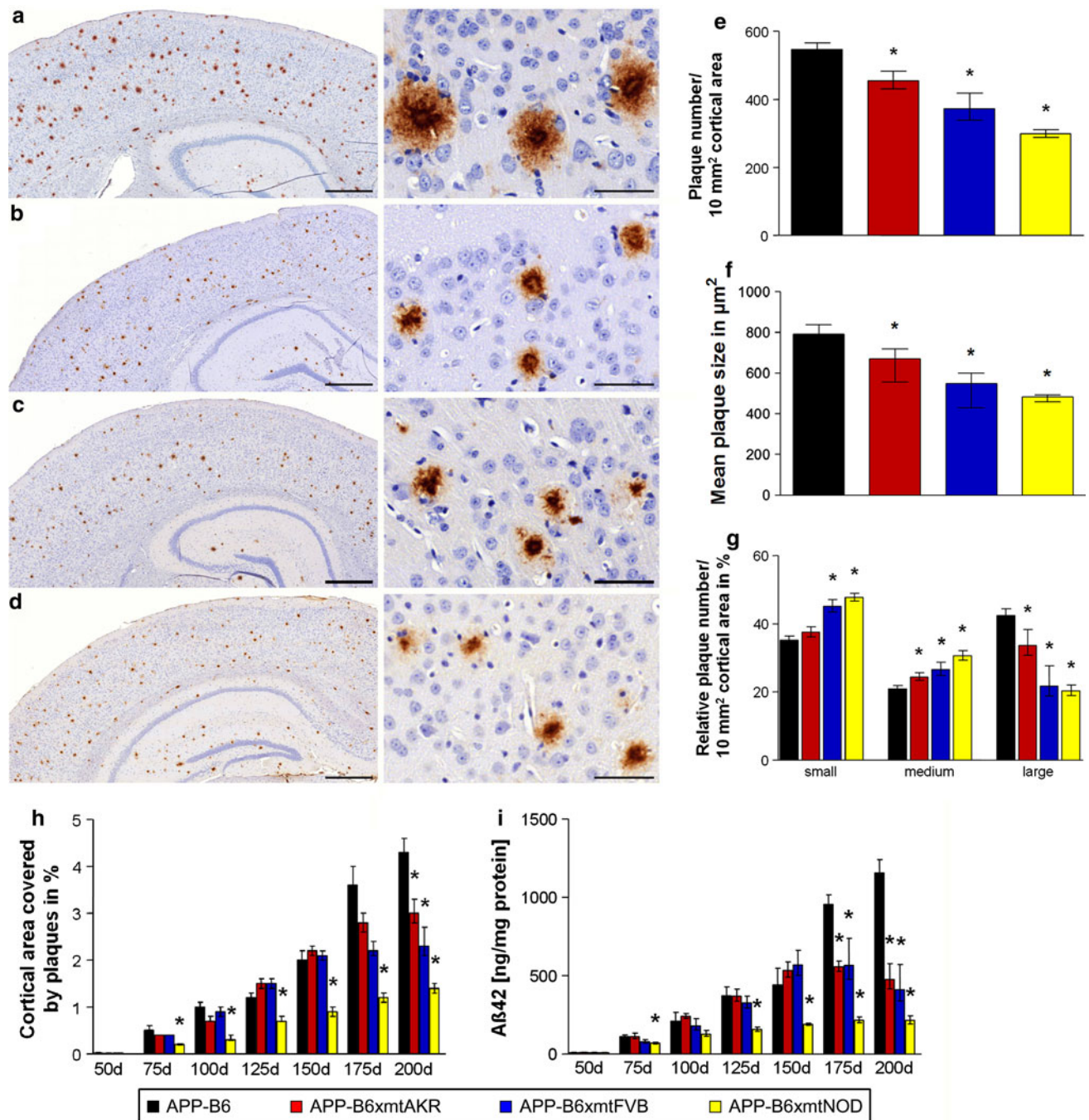


Fig. 2 Mitochondrial modifications in APP-expressing inbred strains strongly influence the deposition of cerebral A β . (**a–d**) Representative immunohistochemical stainings of A β in the transgenic mouse strains (**a** APP-B6, **b** APP-B6xmt^{AKR}, **c** APP-B6xmt^{FVB} and **d** APP-B6xmt^{NOD}), all 200 days of age, demonstrate different plaque sizes. Scale bars represent 500 μ m (*left* photos) and 50 μ m (*right* photos). **e** A significantly lower A β plaque burden compared to APP-B6 was

found in the mtDNA mouse lines at 200 days of age. **f, g** Mean cortical plaque size is reduced because of significantly fewer large plaques. **h** In the APP-B6xmt^{NOD} strain, the cortical area occupied by plaques is significantly less at 75 days of age, and by approximately 175 days of age, it is reduced in all congenic mtDNA mice. **i** The histopathological findings are confirmed by A β 42-ELISA. Data are means \pm SEM ($n \geq 5$ per group), * $p < 0.05$

cerebral A β load, demonstrated significantly higher uptake levels in microglia compared to B6 controls (Fig. 3h). These findings suggest that ATP-triggered microglial activity plays an important role in A β homeostasis.

High ATP levels reduce A β load

The most striking effects in A β reduction are found in mt^{NOD} mice compared to mt^{AKR}, mt^{FVB} and B6 control

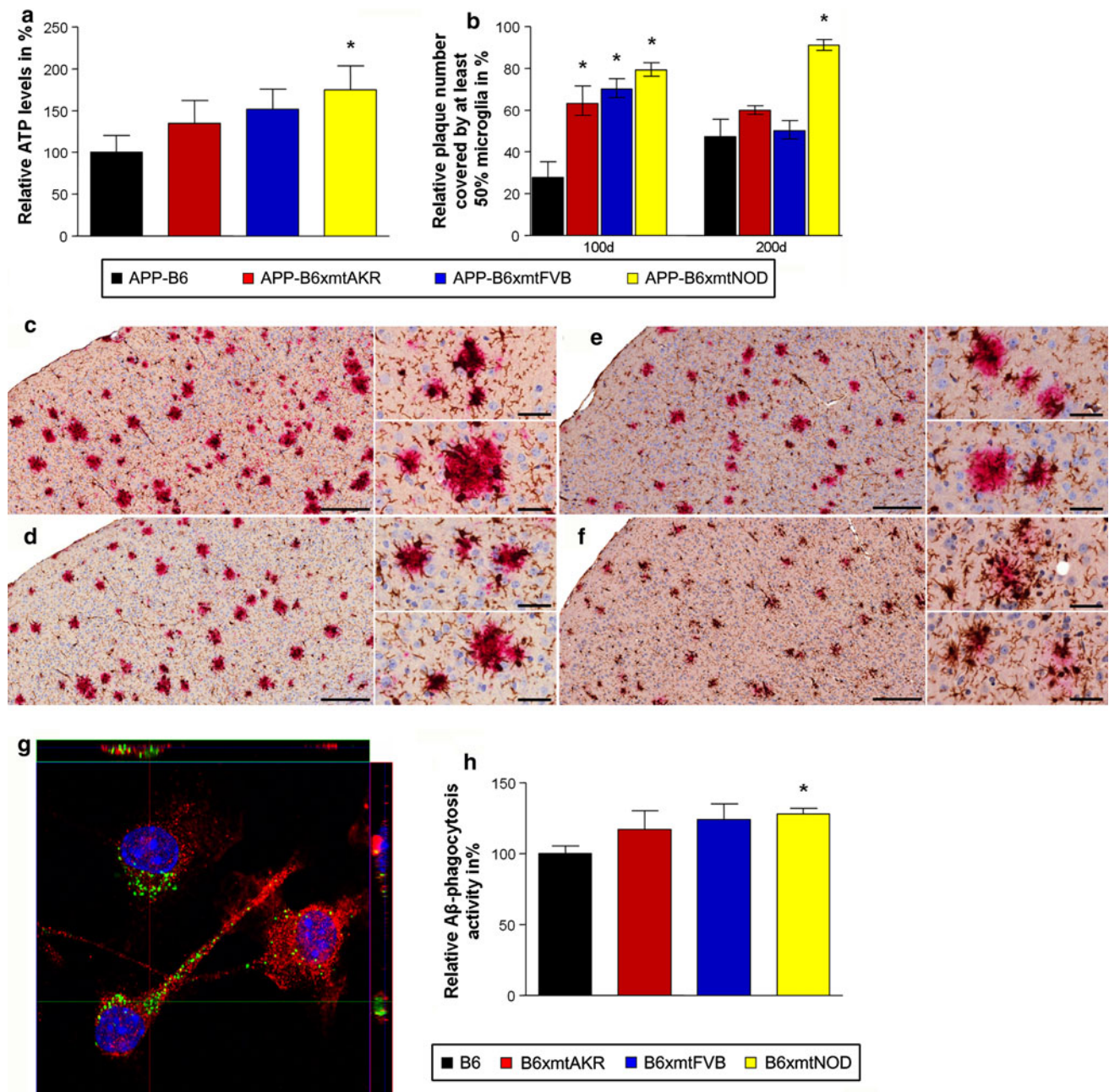


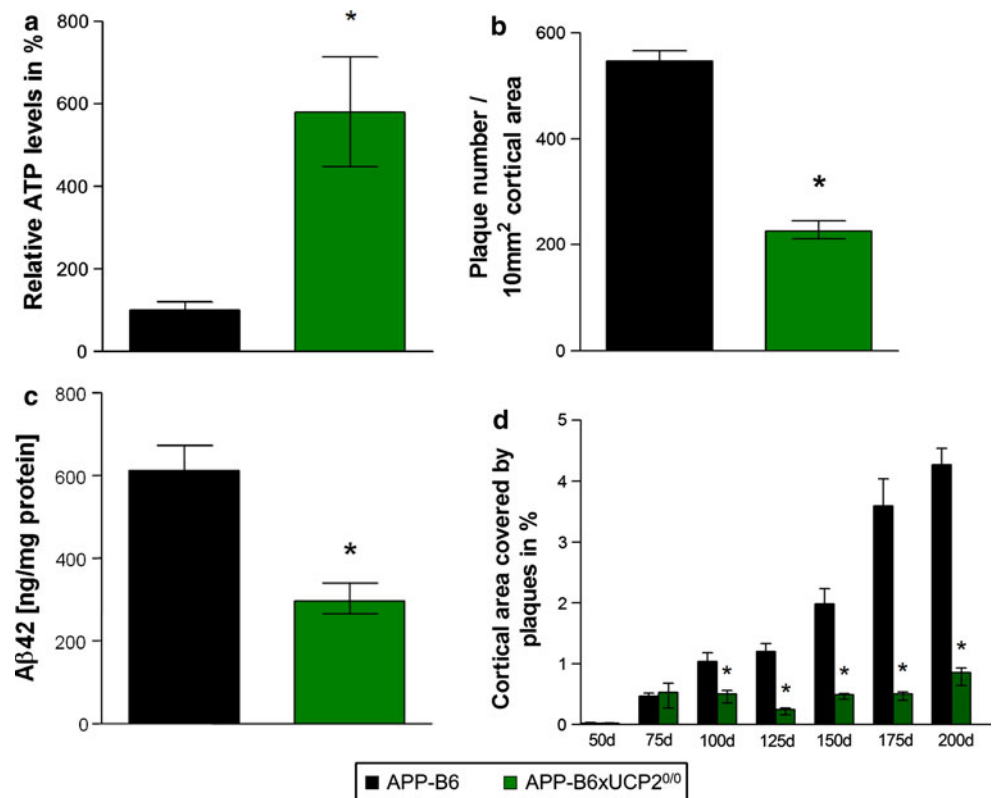
Fig. 3 Increased microglial activation is associated with lower levels of A β in congenic mtDNA mice. **a** Cellular ATP levels are significantly increased in APP-B6xmt^{NOD} mice and moderately, but non-significantly, elevated in the mt^{AKR} and mt^{FVB} strains compared to controls at 200 days of age ($n \geq 10$ per group). **b** The relative number of plaques that are more than 50 % covered by microglia is significantly elevated in the congenic mice at 100 days and remains significantly increased only in the mtNOD mice at the age of 200 days. Data are means \pm SEM ($n \geq 6$ per group), * $p < 0.05$. **c–f** Representative immunohistochemical double-labeling of

Iba1-positive microglia and cerebral A β in the **c** APP-B6, **d** APP-B6xmt^{AKR}, **e** APP-B6xmt^{FVB} and **f** APP-B6xmt^{NOD} mice at 200 days of age reveals substantial reactive microgliosis, most notably in the mt^{NOD} mouse line. Scale bars represent 200 μ m (left photos) and 20 μ m (right photos). **g** Fluorescence image of Iba1-stained microglia (red) demonstrates phagocytosis of fluorescein-labeled synthetic A β 42 (green). **h** In vitro phagocytosis of A β is significantly higher (+28 %) in microglia from B6 \times mt^{NOD} than from B6 control mice. Data are means \pm SEM of three independent experiments ($n \geq 5$ each), * $p < 0.05$

mice. Interestingly, these mice also exhibit the highest ATP levels. It is known that release of ATP triggers microglial response, and this might therefore explain amplified microglial activity toward aggregated A β [7, 8]. To support

the ATP dependency of this phenomenon, we additionally established an mtDNA-independent AD model lacking the nuclear genome-encoded ATP-bypass enzyme uncoupling protein 2 (APP \times UCP^{0/0}). Higher levels of ATP have

Fig. 4 ATP-driven reductions of A β levels in the mtDNA-independent APP-B6 \times UCP2^{0/0} mouse model at 200 days of age. **a** ATP levels are significantly increased by \sim 6-fold in APP-B6 \times UCP2^{0/0} mice. **b** Mean plaque number is reduced by 59 % relative to APP-B6 controls. **c** APP-B6 \times UCP2^{0/0} mice show a significant 52 % reduction in A β 42. **d** The cortical area occupied by amyloid plaques is significantly reduced in the APP-UCP^{0/0} strain starting already at 100 days of age. Data are presented as means \pm SEM ($n \geq 5$ per group), * $p < 0.05$



been observed in various cells types of UCP2-deficient mice [19, 39]. As expected, the APP \times UCP^{0/0} mice also exhibit much higher ATP levels. Most importantly, these mice have significantly lower A β levels in the brain (Fig. 4), which suggests an inverse correlation of increased ATP and reduced A β levels.

Discussion

In this study, we analyzed conplastic mouse models with identical nuclear but divergent mitochondrial genomes, and thereby provide the first in vivo evidence that specific mtDNA variants in common inbred mouse strains can substantially influence the cerebral proteostasis network, indicating a potential role of mtDNA mutations in the ontogeny of neurodegenerative diseases. In particular, we found distinct biochemical alterations resulting in higher ATP levels, lower plaque number and size, lower A β levels and a pronounced microglial response to A β . Energetic differences influence the phagocytic activity of microglia toward A β , which is necessary for plaque removal; hence, the microglial activation state may be an important regulator of the progression of cerebral A β amyloidosis. In line with this, ablation of the majority of parenchymal microglia in one study suggested that amyloid formation and maintenance are not dependent on the presence of

microglia in APP-transgenic mice on a B6 genomic background that miss the energetic phagocytic microglial activation [13]. Senescence leads to the accumulation of random mitochondrial changes in cells and tissues and to an age-related switch in microglial function from phagocytic to more cytotoxic in vivo [16, 31]. Increased heteroplasmy of random mitochondrial polymorphisms accumulating with age could engender gross functional and regulational deficiencies in specific mitochondrial pathways, thus contributing to functional changes of ATP-consuming mechanisms, e.g., A β export from the brain [3, 21, 25], fostering sporadic forms of AD. Consequently, no specific, inherited mtDNA variations have yet been discovered as linked to AD, although several studies have sought to ascertain the presence of mtDNA polymorphisms and maternal inheritance in AD patients [4, 5, 27, 34, 37]. The FVB/N and AKR/J strains have a double and the NOD/LtJ a treble A-repeat. Mutations in *mtRNA^{Arg}* result in an altered conformation and OXPHOS deficiencies in patients [32]. Moreover, alterations of regulatory mechanisms, such as a reduction in the amount of transcripts of NADH dehydrogenase subunits, have been proposed as potential risk factors for AD [5].

Together, ATP level alterations due to functional variations in OXPHOS and/or TCA cycle variations that are caused by accumulating mtDNA mutations lead to beneficial or detrimental effects for the brain's proteostasis

networks and may thus play an important role in the development or even prevention of age-related neurodegenerative diseases.

Acknowledgments The authors thanks K. Nakamura and J. Götz for comments on the manuscript, and Thomas Brüning, Anne-Sophie Plath and Franziska Alfen for technical support. This work was supported by grants from the county of Mecklenburg-Western Pomerania (LGF funding to K.S. and J.S., Excellence Initiative 69027037/290100/2010—UR 09 020 to J.P.), INF Rostock (to M.K.), NIH (RR-00165) and the CART Foundation (to L.C.W.) and the German Science Foundation (DFG ExC 306/1, to S.I.).

Conflict of interest The authors declare that they have no competing financial interests.

References

1. Avise JC, Lansman RA, Shade RO (1979) The use of restriction endonucleases to measure mitochondrial DNA sequence relatedness in natural populations. I. Population structure and evolution in the genus *Peromyscus*. *Genetics* 92(1):279–295
2. Barrientos A, Fontanesi F, Diaz F (2009) Evaluation of the mitochondrial respiratory chain and oxidative phosphorylation system using polarography and spectrophotometric enzyme assays. In: Jonathan L Haines et al (eds) *Current protocols in human genetics/editorial board*. Chap 19:Unit 19.13
3. Bateman RJ (2010) Amyloid-beta production and clearance rates in Alzheimer's disease. *Alzheimer's Dementia* 6(4):S101
4. Chinnery PF, Taylor GA, Howell N, Brown DT, Parsons TJ, Turnbull DM (2001) Point mutations of the mtDNA control region in normal and neurodegenerative human brains. *Am J Hum Genet* 68(2):529–532
5. Coskun PE, Beal MF, Wallace DC (2004) Alzheimer's brains harbor somatic mtDNA control-region mutations that suppress mitochondrial transcription and replication. *Proc Natl Acad Sci USA* 101(29):10726–10731
6. Cottrell DA, Turnbull DM (2000) Mitochondria and ageing. *Curr Opin Clin Nutr Metab Care* 3(6):473–478
7. Davalos D, Grutzendler J, Yang G, Kim JV, Zuo Y, Jung S, Littman DR, Dustin ML, Gan WB (2005) ATP mediates rapid microglial response to local brain injury in vivo. *Nat Neurosci* 8(6):752–758
8. Dibaj P, Nadrigny F, Steffens H, Scheller A, Hirrlinger J, Schomburg ED, Neusch C, Kirchhoff F (2010) NO mediates microglial response to acute spinal cord injury under ATP control in vivo. *Glia* 58(9):1133–1144
9. Eckert A, Hauptmann S, Scherping I, Meinhardt J, Rhein V, Drose S, Brandt U, Fandrich M, Müller WE, Gotz J (2008) Oligomeric and fibrillar species of beta-amyloid (A beta 42) both impair mitochondrial function in P301L tau transgenic mice. *J Mol Med* 86(11):1255–1267. doi:10.1007/s00109-008-0391-6
10. Eckert A, Schulz KL, Rhein V, Gotz J (2010) Convergence of amyloid-beta and tau pathologies on mitochondria in vivo. *Mol Neurobiol* 41(2–3):107–114. doi:10.1007/s12035-010-8109-5
11. Edgar D, Shabalina I, Camara Y, Wredenberg A, Calvaruso MA, Nijtmans L, Nedergaard J, Cannon B, Larsson NG, Trifunovic A (2009) Random point mutations with major effects on protein-coding genes are the driving force behind premature aging in mtDNA mutator mice. *Cell Metab* 10(2):131–138
12. Elson JL, Herrnstadt C, Preston G, Thal L, Morris CM, Edwardson JA, Beal MF, Turnbull DM, Howell N (2006) Does the mitochondrial genome play a role in the etiology of Alzheimer's disease? *Hum Genet* 119(3):241–254
13. Grathwohl SA, Kalin RE, Bolmont T, Prokop S, Winkelmann G, Kaeser SA, Odenthal J, Radde R, Eldh T, Gandy S, Aguzzi A, Staufenbiel M, Mathews PM, Wolburg H, Heppner FL, Jucker M (2009) Formation and maintenance of Alzheimer's disease beta-amyloid plaques in the absence of microglia. *Nat Neurosci* 12(11):1361–1363
14. Hanisch UK, Kettenmann H (2007) Microglia: active sensor and versatile effector cells in the normal and pathologic brain. *Nat Neurosci* 10(11):1387–1394
15. Horvath RJ, Nutile-McMenemy N, Alkaitis MS, Deleo JA (2008) Differential migration, LPS-induced cytokine, chemokine, and NO expression in immortalized BV-2 and HAPI cell lines and primary microglial cultures. *J Neurochem* 107(2):557–569
16. Jimenez S, Baglietto-Vargas D, Caballero C, Moreno-Gonzalez I, Torres M, Sanchez-Varo R, Ruano D, Vizuete M, Gutierrez A, Vitorica J (2008) Inflammatory response in the hippocampus of PS1M146L/APP751SL mouse model of Alzheimer's disease: age-dependent switch in the microglial phenotype from alternative to classic. *J Neurosci* 28(45):11650–11661. doi:28/45/1165010.1523/JNEUROSCI.3024-08.2008
17. Johnson KR, Zheng QY, Bykhovskaya Y, Spirina O, Fischel-Ghodsian N (2001) A nuclear-mitochondrial DNA interaction affecting hearing impairment in mice. *Nat Genet* 27(2):191–194
18. Khan SM, Cassarino DS, Abramova NN, Keeney PM, Borland MK, Trimmer PA, Krebs CT, Bennett JC, Parks JK, Swerdlow RH, Parker WD Jr, Bennett JP Jr (2000) Alzheimer's disease cybrids replicate beta-amyloid abnormalities through cell death pathways. *Ann Neurol* 48(2):148–155
19. Krauss S, Zhang CY, Lowell BB (2002) A significant portion of mitochondrial proton leak in intact thymocytes depends on expression of UCP2. *Proc Natl Acad Sci USA* 99(1):118–122. doi:10.1073/pnas.012410699012410699
20. Krishnan KJ, Greaves LC, Reeve AK, Turnbull DM (2007) Mitochondrial DNA mutations and aging. *Ann N Y Acad Sci* 1100:227–240
21. Krohn M, Lange C, Hofrichter J, Scheffler K, Stenzel J, Steffen J, Schumacher T, Brüning T, Plath AS, Alfen F, Schmidt A, Winter F, Rateitschak K, Wree A, Gsponer J, Walker LC, Pahnke J (2011) Cerebral amyloid-beta proteostasis is regulated by the membrane transport protein ABCC1 in mice. *J Clin Invest* 121(10):3924–3931
22. Larsson NG (2010) Somatic mitochondrial DNA mutations in mammalian aging. *Annu Rev Biochem* 79:683–706
23. Lesné S, Koh MT, Kotilinek L, Kaye R, Glabe CG, Yang A, Gallagher M, Ashe KH (2006) A specific amyloid-beta protein assembly in the brain impairs memory. *Nature* 440(7082):352–357
24. Lin MT, Beal MF (2006) Mitochondrial dysfunction and oxidative stress in neurodegenerative diseases. *Nature* 443(7113):787–795
25. Mawuenyega KG, Sigurdson W, Ovod V, Munsell L, Kasten T, Morris JC, Yarasheski KE, Bateman RJ (2010) Decreased clearance of CNS beta-amyloid in Alzheimer's disease. *Science* 330(6012):1774. doi:science.119762310.1126/science.1197623
26. Moreno-Loshuertos R, Acin-Perez R, Fernandez-Silva P, Movilla N, Perez-Martos A, Rodriguez de Cordoba S, Gallardo ME, Enriquez JA (2006) Differences in reactive oxygen species production explain the phenotypes associated with common mouse mitochondrial DNA variants. *Nat Genet* 38(11):1261–1268
27. Mosconi L, Berti V, Swerdlow RH, Pupi A, Duara R, de Leon M (2010) Maternal transmission of Alzheimer's disease: prodromal metabolic phenotype and the search for genes. *Hum Genomics* 4(3):170–193 (pii:5T232214021U2841)
28. Perry VH, Nicoll JA, Holmes C (2010) Microglia in neurodegenerative disease. *Nat Rev* 6(4):193–201

29. Radde R, Bolmont T, Kaeser SA, Coomaraswamy J, Lindau D, Stoltze L, Calhoun ME, Jaggi F, Wolburg H, Gengler S, Haass C, Ghetti B, Czech C, Holscher C, Mathews PM, Jucker M (2006) Abeta42-driven cerebral amyloidosis in transgenic mice reveals early and robust pathology. *EMBO Rep* 7(9):940–946
30. Roubertoux PL, Sluyter F, Carlier M, Marcet B, Maarouf-Veray F, Cherif C, Marican C, Arrechi P, Godin F, Jamon M, Verrier B, Cohen-Salmon C (2003) Mitochondrial DNA modifies cognition in interaction with the nuclear genome and age in mice. *Nat Genet* 35(1):65–69
31. Scheffler K, Stenzel J, Krohn M, Lange C, Hofrichter J, Schumacher T, Bruning T, Plath AS, Walker L, Pahnke J (2011) Determination of spatial and temporal distribution of microglia by 230 nm-high-resolution, high-throughput automated analysis reveals different amyloid plaque populations in an APP/PS1 mouse model of Alzheimer's disease. *Curr Alzheimer Res* 8(7):781–788. doi:[BSP/CAR/0134](https://doi.org/10.1007/s11434-011-0134-4)
32. Smits P, Mattijssen S, Morava E, van den Brand M, van den Brandt F, Wijburg F, Pruijn G, Smeitink J, Nijtmans L, Rodenburg R, van den Heuvel L (2010) Functional consequences of mitochondrial tRNA Trp and tRNA Arg mutations causing combined OXPHOS defects. *Eur J Hum Genet* 18(3):324–329
33. Swerdlow RH, Parks JK, Cassarino DS, Maguire DJ, Maguire RS, Bennett JP Jr, Davis RE, Parker WD Jr (1997) Cybrids in Alzheimer's disease: a cellular model of the disease? *Neurology* 49(4):918–925
34. Tanaka N, Goto Y, Akanuma J, Kato M, Kinoshita T, Yamashita F, Tanaka M, Asada T (2010) Mitochondrial DNA variants in a Japanese population of patients with Alzheimer's disease. *Mitochondrion* 10(1):32–37
35. Wallace DC (1999) Mitochondrial diseases in man and mouse. *Science* 283(5407):1482–1488
36. Wallace DC, Fan W (2009) The pathophysiology of mitochondrial disease as modeled in the mouse. *Genes Dev* 23(15):1714–1736
37. Wang PN, Lee HC, Wang CH, Ping YH, Liu TY, Chi CW, Lin KN, Liu HC (2009) Heteroplasmy of mitochondrial D310 mononucleotide repeat region in the blood of patients with Alzheimer's disease. *J Alzheimers Dis* 18(2):345–353
38. Yu X, Wester-Rosenlof L, Gimsa U, Holzhuetter SA, Marques A, Jonas L, Hagenow K, Kunz M, Nizze H, Tiedge M, Holmdahl R, Ibrahim SM (2009) The mtDNA nt7778 G/T polymorphism affects autoimmune diseases and reproductive performance in the mouse. *Hum Mol Genet* 18(24):4689–4698
39. Zhang CY, Baffy G, Perret P, Krauss S, Peroni O, Grujic D, Hagen T, Vidal-Puig AJ, Boss O, Kim YB, Zheng XX, Wheeler MB, Shulman GI, Chan CB, Lowell BB (2001) Uncoupling protein-2 negatively regulates insulin secretion and is a major link between obesity, beta cell dysfunction, and type 2 diabetes. *Cell* 105(6):745–755